

Cite this: *RSC Adv.*, 2017, 7, 31771

# Adsorption behavior of the copolymer AM/DMC/APEG/DMAAC-16 on a carbonate rock and its application for acidizing†

Hongping Quan,<sup>ab</sup> Zhonghao Chen,<sup>ab</sup> Yang Wu <sup>\*ab</sup> and Zhuoke Li<sup>ab</sup>

In this study, a quadriopolymer of acrylamide (AM), [2-(methacryloyloxy)ethyl]-trimethylammonium chloride (DMC), allyl polyethylene glycol (APEG), and hexadecyl trimethyl allylammonium chloride (DMAAC-16) was designed and synthesized, which was named PADAD. The molecular structure of PADAD was characterized by Fourier transform infrared (FT-IR) and nuclear magnetic resonance (<sup>1</sup>H-NMR) spectroscopy. The molecular weight and the dispersion exponent of PADAD were determined by gel permeation chromatography (GPC). The adsorption behavior of PADAD on a carbonate rock surface was investigated. The kinetic model of PADAD on a carbonate rock surface was found to fit the pseudo-second-order kinetic model. The adsorption isotherm model of PADAD on the surface of a carbonate rock fitted with the Freundlich model. Addition of PADAD into 20% HCl obviously reduced the rate of the acid rock reaction. We analyzed the microstructure of the rock surface by scanning electron microscopy (SEM) and found that an adsorption film appeared on the rock surface due to PADAD, which could reduce the contact of acid with the rock surface.

Received 10th April 2017

Accepted 6th June 2017

DOI: 10.1039/c7ra04069e

rsc.li/rsc-advances

## Introduction

Due to the fact that long chain alkyl and other lipophilic groups can associate in water, introduction of hydrophobic groups into hydrophilic polymers will change the adsorption behavior of the original polymers.<sup>1–3</sup> Commonly, water-soluble polymers, such as polyacrylamide, can form a monolayer upon adsorption.

However, polymers with a hydrophobic group could present adsorption of a multilayer. Since hydrophobic association existed between molecules, the polymer could be adsorbed on the already formed adsorption layer.<sup>4–6</sup> Recently, hydrophobic associating polymers have been widely used in oilfield applications, such as acidizing treatments,<sup>7,8</sup> drilling and completion fluids, and polymer flooding.<sup>9–12</sup> In oilfield applications, the hydrophobic associating polymer is adsorbed on the reservoir for the interaction of the polymer and the reservoir, which may have some effect on the reservoir. The adsorption behavior of hydrophobic associating polymers has attracted significant attention from many researchers. Some researchers have researched the adsorption behavior of these polymers on clay particles and silica sand.<sup>5,13</sup> However, the study on the

adsorption behavior between hydrophobic associative polymers and carbonates has not yet been perfected, especially the study of the adsorption capacity and adsorption rate. Therefore, the study on the adsorption behavior of hydrophobic associative polymers on carbonate rocks was very important, which could provide a theoretical basis for the practical application of hydrophobic associative polymers in oil and gas exploration.

In our study, a quadriopolymer, PADAD, was synthesized using acrylamide (AM), [2-(methacryloyloxy)ethyl]-trimethylammonium chloride (DMC), allyl polyethylene glycol (APEG), and hexadecyl trimethyl allylammonium chloride (DMAAC-16) through free radical polymerization. The aim of this study was to research the adsorption behavior, including the effect of external factors, the adsorption isotherm model, and the kinetic model, of PADAD on a carbonate rock. Through this research, we could provide theoretical support for PADAD applications in the future.

## Experimental

### Materials

Chemically pure AM, DMC, and 2,2'-azobis[2-methylpropanamide]dihydrochloride (AIBA) were produced by Chengdu Chang-zheng Glass Co., Ltd. (China). Industrial grade APEG-1000 was produced by Jiangsu Hai-an Petrochemical Factory (China). Industrial grade DMAAC-16 was produced by Jiangsu Fu-Miao Technology Co., Ltd. (China).

<sup>a</sup>College of Chemistry and Chemical Engineering, Southwest Petroleum University, No. 8 Xindu Road, Chengdu 610500, P. R. China. E-mail: wuyang1119@hotmail.com; Fax: +86-28-83037305; Tel: +86-28-83037305

<sup>b</sup>Oil & Gas Field Applied Chemistry Key Laboratory of Sichuan Province, Southwest Petroleum University, Chengdu, P. R. China

† Electronic supplementary information (ESI) available. See DOI: 10.1039/c7ra04069e



## Synthesis

In this experiment, the  $n(\text{AM}) : n(\text{APEG}) : n(\text{DMC}) : n(\text{DMAAC-16})$  ratio was 20.00 : 1.00 : 4.00 : 0.14.

First, 5 g (0.07 mol) AM was dissolved in 27.18 g (1.51 mol) deionized water in a three-necked flask. Second, 0.16 g (0.0005 mol) DMAAC-16, 3.52 g (0.0035 mol) APEG, and 2.92 g (0.014 mol) DMC were transferred into the previous solution and stirred until the mixed solution was completely dissolved. Third, the solution was bubbled with  $\text{N}_2$  for 30 minutes, and then, 0.0223 g of initiator (AIBA) was added into the solution. The reaction lasted 6 h at 60 °C, and a crude product was obtained.

The crude product was purified by ethanol and then dried in a vacuum drying oven at 40 °C. The molecular structure of PADAD is displayed in Scheme 1.

## Characterization

The determination of the molecular weight and the distribution of PADAD were tested by GPC (Waters e2695, USA). PADAD was dissolved into a sodium nitrate solution (0.1 mol  $\text{L}^{-1}$ ), and the concentration of PADAD was 2 mg  $\text{mL}^{-1}$ .

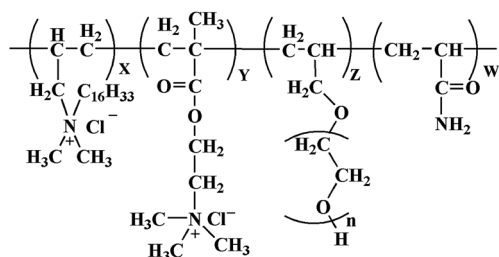
Through mixing the PADAD and KBr powder together and squashing by a tablet machine, the samples were obtained and then measured *via* FTIR (WQF-520, Beijing Beifen-Ruili Analytical Instrument (Group) Co., Ltd, China) in the range between 4000 and 500  $\text{cm}^{-1}$ .

PADAD was dissolved in  $\text{D}_2\text{O}$ , and then, the structural characterization of the PADAD was carried out by  $^1\text{H-NMR}$  (Bruker-400, Bruker, Germany).

The change in micro-morphology of a carbonate rock was observed during the process of acid treatment *via* scanning electron microscopy (JSM7500F, Japan).

## Adsorption measurements

The depletion method was used to determine the adsorption of PADAD on a carbonate rock.<sup>13</sup> Rock particles were added to different concentrations of PADAD solution and oscillated by a constant temperature oscillator under different experimental conditions until adsorption equilibrium was reached. Through the difference in the concentrations of PADAD in the initial and final solutions, the adsorption of PADAD was obtained. The concentration of PADAD in different solutions was measured by a total organic carbon analyzer (TOC-VCPH, Shimadzu



Scheme 1 Molecular structure of PADAD.

Corporation, Japan). During the measurement of adsorption, the solid/liquid weight ratio (S/L) was 0.1.

In the adsorption isotherm experiments, we researched the adsorption state and strength of PADAD on a carbonate rock. The volume of the PADAD solution was 20 mL, and the mass of the carbonate particles was 2 g. We determined the equilibrium adsorption capacity of PADAD of different initial concentrations at the same temperature. The initial concentration of PADAD ranged from 1000 mg  $\text{L}^{-1}$  to 12 000 mg  $\text{L}^{-1}$ , and the experimental temperature was 30 °C, 50 °C, and 70 °C.

In the adsorption kinetics experiments, we first researched the effect of oscillating time on the adsorption of PADAD. The volume of the PADAD solution was 20 mL, and the mass of the carbonate particles was 2 g. We calculated the adsorption of PADAD every 5 minutes until the adsorption reached equilibrium; the initial concentrations of PADAD were 3000 mg  $\text{L}^{-1}$ , 5000 mg  $\text{L}^{-1}$ , 7000 mg  $\text{L}^{-1}$ , and 9000 mg  $\text{L}^{-1}$  at 30 °C.

Moreover, we also researched the effect of temperature on the adsorption of PADAD. The volume of the PADAD solution was 20 mL, and the mass of the carbonate particles was 2 g. We calculated the adsorption of PADAD every 5 minutes until the adsorption reached equilibrium. The initial concentration of PADAD was 7000 mg  $\text{L}^{-1}$  and the experimental temperatures were 30 °C, 50 °C, and 70 °C.

## Retarding capability test of PADAD

Different masses of PADAD were added to 20% HCl, and the resulting solution was named PADAD acid. The retarding capability of PADAD was determined by the reaction rate of carbonate and PADAD acid. The experimental temperature was 30 °C, and the reaction area was 5  $\text{cm}^2$ . The reaction rate was tested and calculated according to literature.<sup>8</sup>

## Results and discussion

### Characterization of PADAD

The synthesized sample was analyzed by FT-IR after purification, and the result is displayed in Fig. 1.

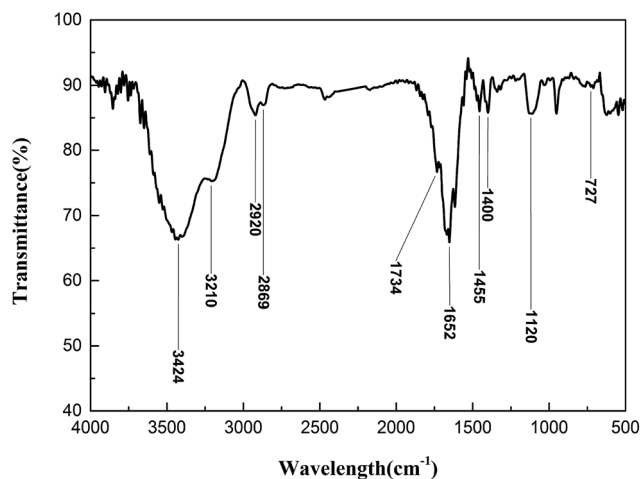


Fig. 1 FTIR spectra of PADAD.



As shown in Fig. 1, there is a peak at  $3424\text{ cm}^{-1}$  attributed to the stretching vibration peak of N–H. The peak at  $3210\text{ cm}^{-1}$  illustrated that a hydroxyl group existed in PADAD. The peaks at  $2920\text{ cm}^{-1}$  and  $2869\text{ cm}^{-1}$  are the stretching vibrations of C–H from methyl and methylene, respectively. The peak at  $1734\text{ cm}^{-1}$  indicates that the carbonyl group from DMC exists in PADAD. The peak at  $1652\text{ cm}^{-1}$  indicates that the carbonyl group from AM exists in PADAD. The peak at  $1455\text{ cm}^{-1}$  is the bending vibration peaks of C–H. The peak at  $1400\text{ cm}^{-1}$  illustrates that C–N from the amide group exists in PADAD. The peak at  $1120\text{ cm}^{-1}$  illustrates that the ether bond from APEG exists in PADAD. The peak at  $727\text{ cm}^{-1}$  illustrates that  $(\text{CH}_2)_{15}$  from DMAAC-16 exists in PADAD.

The molecular weight of PADAD and its distribution were tested, and the result is shown in Table 1.

Table 1 shows that the weight average molecular weight ( $M_w$ ) was  $1.22 \times 10^5$ , and the number average molecular weight ( $M_n$ ) was  $6.58 \times 10^4$ . Thus, the molecular weight distribution coefficient is 1.85. These all meet the technical requirements for oilfield application.

$^1\text{H-NMR}$  spectrum of PADAD is shown in Fig. 2.

$^1\text{H-NMR}$  (400 MHz,  $\text{D}_2\text{O}$ ):  $\delta = 1.12$ (d,  $-\text{CH}_3$ ),  $\delta = 1.21$ (g, h, i, m, r,  $-\text{CH}_2-$ ,  $-\text{CH}_2-$ ,  $-\text{CH}_3$ ,  $-\text{CH}_2-$ ,  $-\text{CH}_2-$ ),  $\delta = 1.60$ (c,  $-(\text{CH}_2)_{14}-$ ),  $\delta = 1.72$ (n,  $-\text{CH}-\text{CH}_2-\text{O}-$ ),  $\delta = 2.03$ (q,  $-\text{OH}$ ),  $\delta = 2.16$ (f,  $-\text{N}^+-\text{CH}_2-\text{CH}$ ),  $\delta = 2.29$ (s,  $-\text{CH}-(\text{C}=\text{O})-\text{NH}_2$ ),  $\delta = 3.14$ (e,  $-\text{N}^+-\text{CH}_2$ ),  $\delta = 3.18$ (b,  $-\text{N}^+-\text{CH}_2-\text{C}_{15}\text{H}_{31}$ ),  $\delta = 3.45$ (a, l,  $-\text{N}^+-\text{CH}_3$ ),  $\delta = 3.58$ (o,  $-\text{CH}_2-\text{O}-(\text{CH}_2-\text{CH}_2-\text{O})_n-\text{H}$ ),  $\delta = 3.65$ (k, p,  $-\text{N}^+-\text{CH}_2-\text{CH}_2-\text{O}-$ ,  $-(\text{CH}_2-\text{CH}_2-\text{O})_n-\text{H}$ ),  $\delta = 3.99$ (j,  $(\text{C}=\text{O})-\text{O}-\text{CH}_2-$ ).

Table 1 The molecular weight of PADAD

$M_n$	$M_w$	Polydispersity
$6.58 \times 10^4$	$1.22 \times 10^5$	1.85

These features indicated that the obtained product was basically consistent with the designed molecule, which suggested that PADAD was successfully synthesized.

### Adsorption isotherms

In general, the adsorption process of a polymer on a rock is controlled by intermolecular forces such as van der Waals interactions and electrostatic forces.<sup>14</sup> The amount of polymer adsorbed on the surface of the carbonate rock was affected by temperature, salinity, and other external conditions. The adsorption isotherms are displayed in Fig. 3a.

At present, there are many models that could be used to describe the adsorption isotherm model. The Langmuir model and Freundlich model are commonly used to fit the experimental data, which are beneficial to further understand the adsorption behavior.<sup>13,14</sup> The saturated adsorption capacity was determined with an initial concentration of PADAD ranging from  $1000\text{ mg L}^{-1}$  to  $12\,000\text{ mg L}^{-1}$  at 30, 50, and  $70\text{ }^\circ\text{C}$ . The data obtained from the experiments were described by two models.

Langmuir model:

$$\frac{C_e}{Q_e} = \frac{C_e}{Q_m} + \frac{1}{k_L Q_m}$$

In the abovementioned equation,  $Q_e$  ( $\text{mg g}^{-1}$ ) and  $C_e$  ( $\text{mg L}^{-1}$ ) are the adsorption capacity and the residual concentrations of PADAD in the solution at equilibrium, respectively.  $Q_m$  ( $\text{mg g}^{-1}$ ) is the maximum adsorption of PADAD in the solution at equilibrium; the Langmuir constant  $K_L$  ( $\text{L mg}^{-1}$ ) can be used to describe a monolayer adsorption.<sup>15–17</sup> Fig. S1† displays the Langmuir linear plots at 30, 50, and  $70\text{ }^\circ\text{C}$ . The parameters for the adsorption of PADAD onto a carbonate rock are shown in Table S1.†

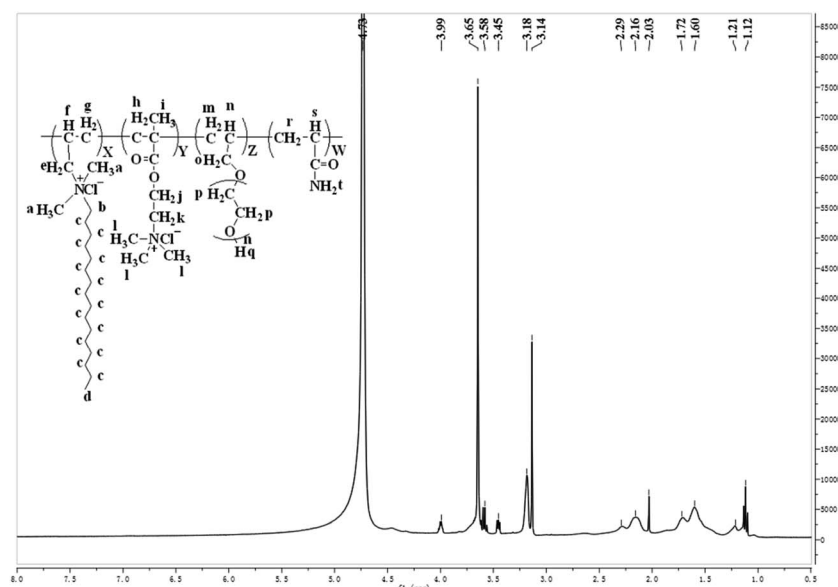


Fig. 2  $^1\text{H-NMR}$  spectra of the polymerization product.



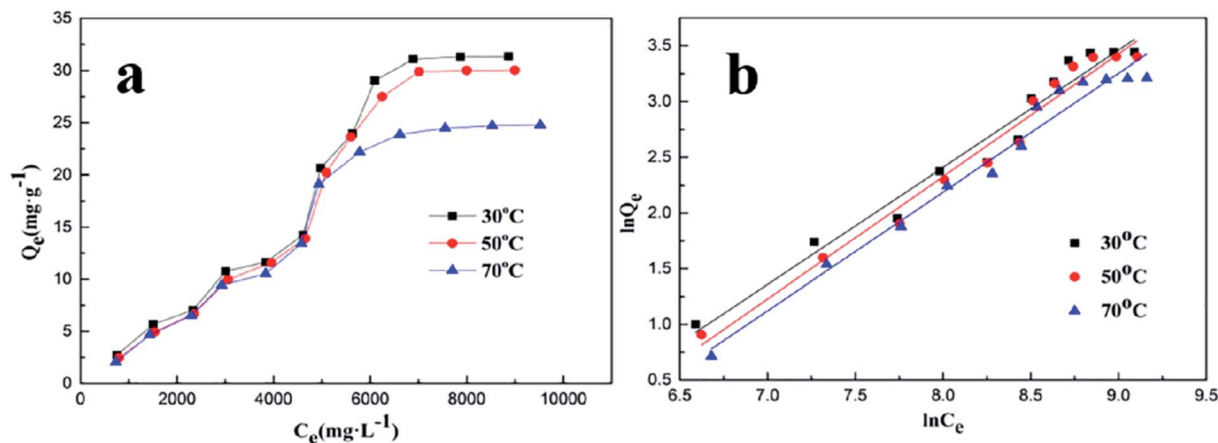


Fig. 3 (a) The adsorption isotherms for PADAD adsorbed on a carbonate rock. (b) Freundlich isotherms for PADAD adsorbed on a carbonate rock.

Freundlich model:

$$\ln Q_e = \frac{1}{n} \ln C_e + \ln K_F$$

In the abovementioned equation,  $C_e$  ( $\text{mg L}^{-1}$ ) and  $Q_e$  ( $\text{mg g}^{-1}$ ) are the concentrations of PADAD in the liquid and solid phases, respectively, when the process of adsorption reaches equilibrium. The Freundlich constant  $K_F$  is related to the adsorption state of the adsorbent, which can be used to describe a multilayer adsorption;  $n$  is the Freundlich constant, which is affected by temperature and can reflect the adsorption strength of the adsorbent.<sup>18</sup> The Freundlich linear plots at different temperatures are displayed in Fig. 3b. The parameters for the adsorption of PADAD onto a carbonate rock are displayed in Table 2.

As can be seen in Tables S1† and 2, the correlation of the curve ( $R^2$ ) of the Freundlich isotherm was obviously much better for PADAD than that of the Langmuir isotherm, which indicated that the process of PADAD adsorption on a carbonate rock could be described by the Freundlich model. During the process of adsorption, extension instead of globosity was observed for PADAD, which means that PADAD can adsorb onto the carbonate directly using many segments within its structure. Moreover, PADAD can be adsorbed onto the previous adsorption layer by intermolecular association; thus, the adsorption of PADAD on the carbonate rock is multilayer adsorption.

Table 2 Freundlich parameters for PADAD adsorbed on a carbonate rock

Temperature (°C)	Freundlich equation	$n$	$K_F$	$R^2$
30	$y = 1.0507x - 5.9984$	0.9517	0.0025	0.9664
50	$y = 1.0990x - 6.4638$	0.9099	0.0016	0.9746
70	$y = 1.0660x - 6.3397$	0.9381	0.0017	0.9734

Furthermore, the process of adsorption was also involved in the dynamic process, which means that adsorption and desorption occurred at the same time.<sup>18,19</sup>

### Adsorption kinetics

The kinetics study of the adsorption process was carried out to investigate the rate and mechanism of adsorption. Currently, there are many kinetic models that have been applied to study the kinetics of the adsorption process, and the pseudo-first-order and pseudo-second-order equation models are widely used.<sup>18,20</sup>

The equation for the pseudo-first-order kinetic model is displayed below:

$$\ln(Q_{e,1} - Q_t) = \ln Q_{e,1} - k_1 t$$

In the abovementioned equation,  $Q_{e,1}$  ( $\text{mg g}^{-1}$ ) is the theoretical capacity of equilibrium adsorption,  $Q_t$  ( $\text{mg g}^{-1}$ ) is the adsorption capacity at time  $t$ , and  $k_1$  is the constant of the pseudo-first-order adsorption kinetic model that can reflect the adsorption rate.

$$\frac{t}{Q_t} = \frac{1}{Q_{e,2}} t + \frac{1}{k_2 Q_{e,2}^2}$$

In this equation,  $Q_{e,2}$  ( $\text{mg g}^{-1}$ ) is the theoretical capacity of equilibrium adsorption,  $Q_t$  ( $\text{mg g}^{-1}$ ) is the adsorption capacity at time  $t$ , and  $k_2$  is the constant of the pseudo-first-order adsorption kinetic model that can reflect the adsorption rate.<sup>17,18</sup>

The curves for the adsorption kinetics at different PADAD concentrations on a carbonate rock are illustrated in Fig. 4a.

As shown in Fig. 4a, the adsorption of PADAD on the surface of a carbonate rock increased with time, and the adsorption was saturated at 60 min. The adsorption process could be divided into the following two phases: fast adsorption and slow adsorption. Fast adsorption occurred during the first 60 min; then, the adsorption slowed down and reached saturation. The saturated adsorption capacity of PADAD on the carbonate rock



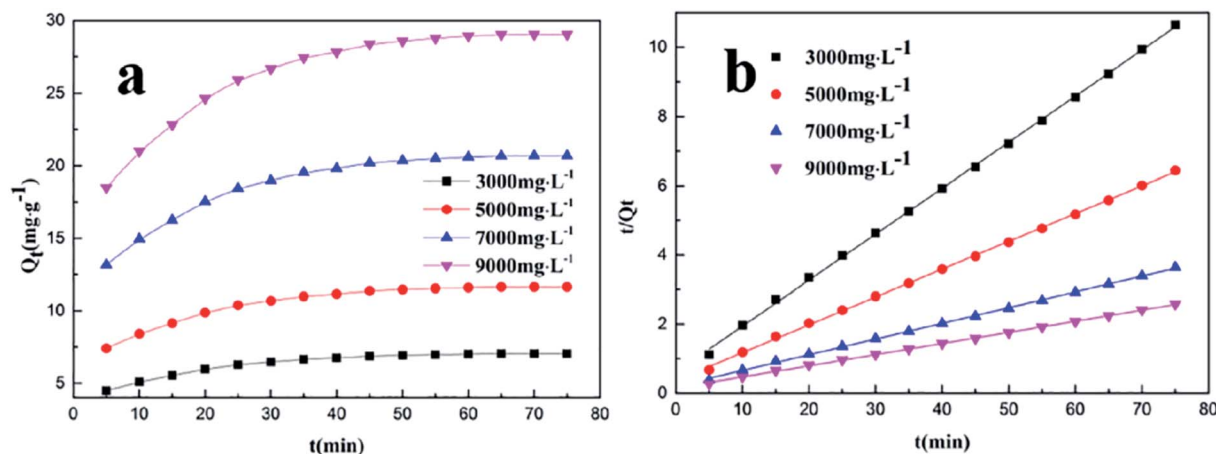


Fig. 4 (a) Effect of the initial concentration on the adsorption of PADAD on a carbonate rock. (b) Pseudo-second-order equation for the adsorption kinetics of PADAD on a carbonate rock.

increased with an increase in the initial concentration of PADAD.

The curves of the pseudo-first-order kinetic equations for the adsorption of PADAD on the carbonate rock at different concentrations are shown in Fig. S2† and the parameters of the equations are illustrated in Table S2.† Moreover, the curves of the pseudo-second-order kinetic equation for the adsorption of PADAD on a carbonate rock at different concentrations are displayed in Fig. 4b, and the parameters of the equations are shown in Table 3.

From the parameters obtained through fitting of the kinetics data from Fig. S2† and 4b and the results displayed in Tables S2† and 3, it was observed that the pseudo-second-order kinetic model was obviously much fitter for the adsorption process than the pseudo-first-order kinetic mode according to the correlation coefficient ( $R^2$ ).

To further study the effect of temperature on the adsorption rate, the adsorption capacity of PADAD on the carbonate rock was investigated at various temperatures, with the results displayed in Fig. 5.

Table 3 Kinetic parameters for the pseudo-second-order equation

Initial concentration (mg L <sup>-1</sup> )	$Q_e$ (mg g <sup>-1</sup> )	Kinetic equation	$R^2$	$Q_{e,2}$ (mg g <sup>-1</sup> )	$k_2$ (mg g <sup>-1</sup> min <sup>-1</sup> )
3000	7.0494	$y = 0.1330x + 0.6107$	0.9995	7.5188	0.0290
5000	11.6421	$y = 0.0805x + 0.3692$	0.9995	12.4224	0.0176
7000	20.6587	$y = 0.0454x + 0.2050$	0.9995	22.0264	0.0101
9000	29.0481	$y = 0.0323x + 0.1481$	0.9995	30.9598	0.0070

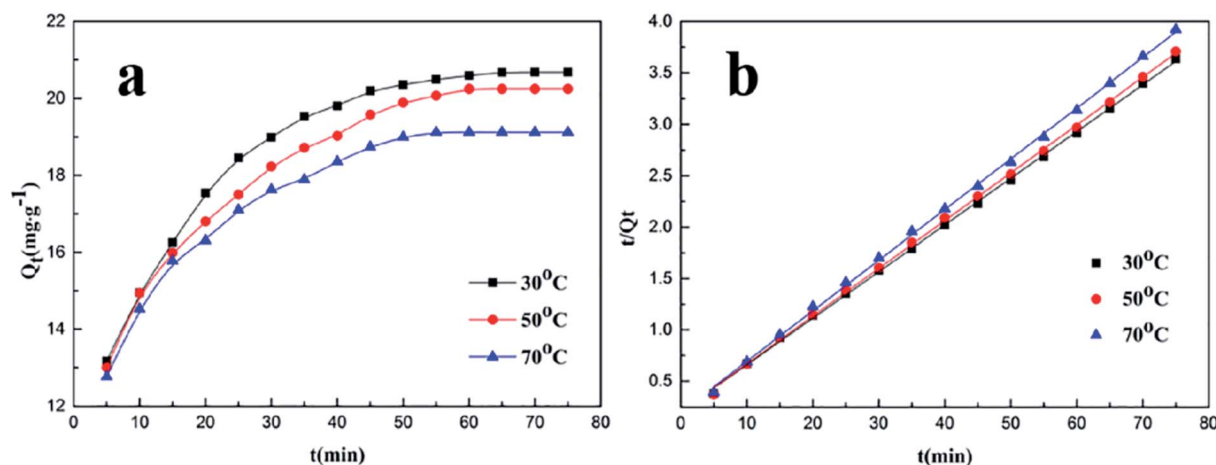


Fig. 5 (a) Effect of temperature on the adsorption of PADAD on a carbonate rock. (b) Pseudo-second-order equation for the adsorption kinetics of PADAD on a carbonate rock at different temperatures.



As seen in Fig. 5a, the adsorption capacity ( $Q_t$ ) decreased with the increasing adsorption temperature in the whole process. Moreover, along with the increasing adsorption temperature, the time to reach adsorption equilibrium was slightly shortened. The results indicate that temperature has a negative influence on the adsorption capacity and has a promoting effect on the adsorption rate.

The curves of the pseudo-first-order kinetic equation for the adsorption of PADAD on the carbonate rock at different temperatures are displayed in Fig. S3,† and the equation parameters are shown in Table S3.† Moreover, the curves of the pseudo-second-order kinetic equation for the adsorption of PADAD on the carbonate rock at different temperatures are shown in Fig. 5, and the parameters of the equations are illustrated in Table 4.

By analyzing the results of kinetic fitting shown in Fig S3† and 5b and the parameters displayed in Tables S3† and 4, it was found that the pseudo-second-order kinetic model was obviously much fitter for the adsorption process than the pseudo-first-order kinetic model at different temperatures according to the correlation coefficient ( $R^2$ ).

As can be seen in Table 4, with the increasing experimental temperature, the adsorption rate increased, but the capacity of equilibrium adsorption was obviously decreased. As above-mentioned, the adsorption process of PADAD on the carbonate rock was dynamic, and the adsorption and desorption occurred at the same time. It means that temperature has a positive influence on both adsorption and desorption but the influence on desorption was larger than that on adsorption. All these results indicated that the adsorption of PADAD on the

carbonate rock was a physical process, in which the time to reach equilibrium was shortened but the adsorption capacity was decreased.<sup>15</sup>

### Retarding capability of PADAD

The retarding capability of PADAD was evaluated by the total volume of  $\text{CO}_2$  produced by the reaction of PADAD acid and carbonate and the reaction rate. The results are displayed in Fig. 6.

Fig. 6a shows that the total volume of  $\text{CO}_2$  decreased with the increasing PADAD concentration. Fig. 6b shows that the reaction rate decreased when PADAD was added into HCl. Moreover, as the concentration of PADAD added into the acid solution was increased, the reaction rate obviously decreased, which indicated that PADAD could retard the acid rock reaction.

The amide group and polyoxyethylene group of PADAD can adsorb onto the surface of the rock by hydrogen bonds.<sup>21,22</sup> Moreover, the quaternary ammonium group with a positive charge in PADAD can adsorb onto the surface of the rock with a large negative charge. A film was formed on the carbonate rock due to the adsorption of PADAD, which could prevent hydrogen ion transfer from the solution to the carbonate rock; thus, the reaction rate was obviously reduced. It illustrates that PADAD has excellent performance in reducing the acid rock reaction rate.

### Mechanism analysis

We treated the carbonate rock *via* different ways and observed its microstructure of *via* SEM. By this way, we could have

Table 4 Kinetic parameters for the pseudo-second-order equation at different temperatures

Temperature ( $^{\circ}\text{C}$ )	$Q_e$ ( $\text{mg g}^{-1}$ )	Kinetic equation	$R^2$	$Q_{e,2}$ ( $\text{mg g}^{-1}$ )	$k_2$ ( $\text{mg g}^{-1} \text{min}^{-1}$ )
30	20.6587	$y = 0.0454x + 0.2050$	0.9995	22.03	$1.01 \times 10^{-2}$
50	20.2566	$y = 0.0465x + 0.2043$	0.9995	21.51	$1.06 \times 10^{-2}$
70	19.1412	$y = 0.0493x + 0.2014$	0.9994	20.28	$1.21 \times 10^{-2}$

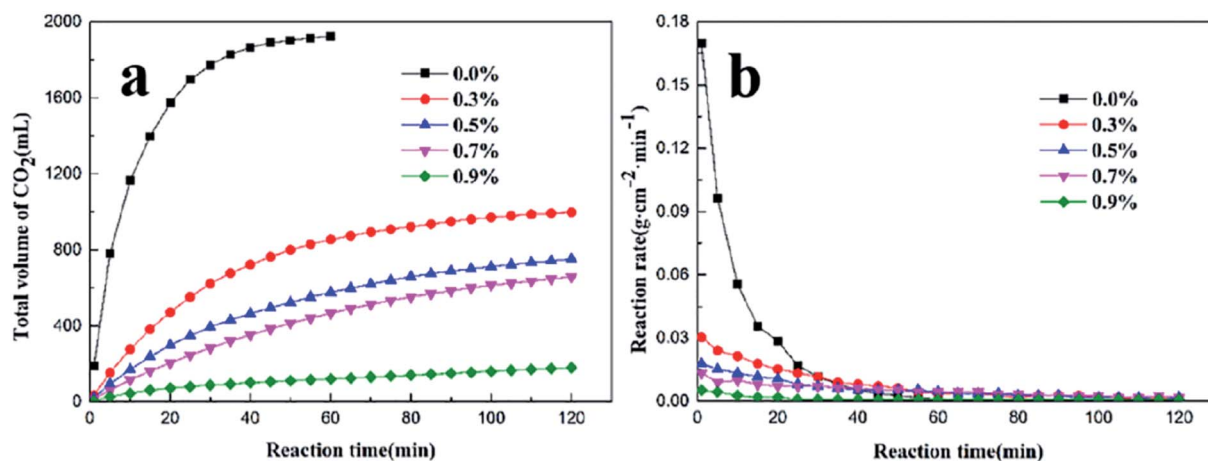


Fig. 6 (a) The total volume of  $\text{CO}_2$  at different concentrations of PADAD in acid. (b) The reaction rate of PADAD acid and the carbonate rock with different concentration of PADAD.



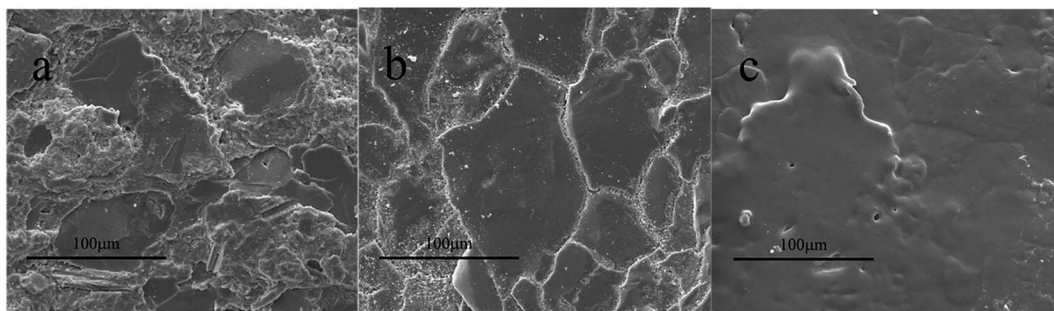


Fig. 7 (a) SEM of an unprocessed carbonate sample. (b) SEM of the carbonate sample treated by 20% HCl. (c) SEM of the carbonate sample treated by PADAD acid.

a better understanding on how PADAD works. The results are displayed as follows.

As shown in Fig. 7a, the surface of the unprocessed carbonate rock was very rough and had a little crack. The carbonate was treated by 20% HCl, and the surface of the carbonate rock was leveled and had many cracks and residues, as shown in Fig. 7b. The carbonate rock was treated by PADAD acid containing 0.7 wt% PADAD, as shown in Fig. 7c. Compared with the carbonate rock surface shown in Fig. 7b, a thin-layer adsorption film can be seen on the carbonate surface shown in Fig. 7c, which can prevent  $H^+$  transfer from the solution to the carbonate surface; furthermore, the reaction rate was reduced.

## Conclusion

In this study, a quadripolymer, PADAD, was synthesized by AM, APEGM, DMC, and DMAAC-16 through free radical polymerization. Through FT-IR and  $^1H$ -NMR, we analyzed the molecular structure of PADAD, and the results illustrated that the structure of PADAD was the same as that of the designed molecule. The weight average molecular weight ( $M_w$ ) was  $1.22 \times 10^5$ , the number average molecular weight ( $M_n$ ) was  $6.58 \times 10^4$ , and the molecular weight distribution coefficient was 1.85.

The adsorption behavior of PADAD on a carbonate rock surface was researched. The kinetic model of PADAD on the carbonate rock surface was fitted by the pseudo-second-order kinetic model. The adsorption isotherm model of PADAD on the carbonate rock surface was fitted by the Freundlich model. PADAD can form a film on the carbonate rock surface, which can prevent  $H^+$  contact with carbonate and reduce the reaction rate. The excellent property of PADAD for reducing the reaction rate of HCl and carbonate illustrates its potential application for acidizing in oil and gas fields. We will do further research on other copolymer applications for acidizing in the future.

## Abbreviations

AM	Acrylamide
DMC	[2-(Methacryloyloxy)ethyl]-trimethylammonium chloride
APEG	Allyl polyethylene glycol

DMAAC-16	Hexadecyl trimethyl allylammonium chloride
PADAD	Copolymer AM/DMC/APEG/DMAAC-16
FT-IR	Fourier transform infrared
$^1H$ -NMR	Nuclear magnetic resonance hydrogen spectrum
GPC	Gel permeation chromatography
SEM	Scanning electron microscopy
AIBA	2,2'-Azobis[2-methylpropionamide] dihydrochloride

## Acknowledgements

This work was supported by the National Natural Science Foundation of China (No. 51604229), the Scientific Research Starting Project of Southwest Petroleum University (No. 2015QHZ015), and the Opening Project of Oil & Gas Field Applied Chemistry Key Laboratory (YQKF201401).

## References

- 1 P. Zhang, W. Huang, Z. Jia, C. Zhou, M. Guo and Y. Wang, *J. Polym. Res.*, 2014, **21**, 522.
- 2 Y. A. Shashkina, Y. D. Zaruslov, V. A. Smirnov, O. E. Philippova, A. R. Khokhlov, T. A. Pryakhina and N. A. Churochkina, *Polymer*, 2003, **44**, 2289.
- 3 P. Zhang, Y. Wang, W. Chen, H. Yu, Z. Qi and K. Li, *J. Solution Chem.*, 2011, **40**, 447.
- 4 L. Eoff, D. Dalrymple and B. R. Reddy, *SPE Prod. Facil.*, 2005, **20**, 250.
- 5 E. Volpert, J. Selb, F. Candau, N. Green, J. F. Argillier and A. Audibert, *Langmuir*, 1998, **14**, 1870.
- 6 K. C. Taylor, and H. A. Nasr-El-Din, *Canadian International Petroleum Conference*, Calgary, June 12–14 2007.
- 7 K. C. Taylor and H. A. Nasr-El-Din, *J. Pet. Sci. Eng.*, 1998, **19**, 265.
- 8 H. Quan, H. Li, Z. Huang and T. Zhang, *J. Appl. Polym. Sci.*, 2015, **132**, 2259.
- 9 A. Audibert and J. F. Argillier, 1998, *U.S. Pat.*, 5, 720 347.
- 10 S. Gou, Y. He, Y. Ma, S. Luo, Q. Zhang, D. Jing and Q. Guo, *RSC Adv.*, 2015, **5**, 51549.
- 11 S. Gou, Y. He, L. Zhou, P. Zhao, Q. Zhang, S. Li and Q. Guo, *New J. Chem.*, 2015, **39**, 9265.



- 12 X. Li, C. Zou and C. Cui, *Starch/Staerke*, 2015, **67**, 673.
- 13 J. F. Argillier, A. Audibert, J. Lecourtier, M. Moan and L. Rousseau, *Colloids Surf., A*, 1996, **113**, 247.
- 14 H. Lu and Z. Huang, *J. Macromol. Sci., Part A: Pure Appl. Chem.*, 2009, **46**, 412.
- 15 Q. Li, Q. Y. Yue, Y. Su, B. Y. Gao and L. Fu, *J. Hazard. Mater.*, 2007, **147**, 370.
- 16 T. Zhang, F. Wu, Z. Xu, Z. Huang and C. Ouyang, *J. Dispersion Sci. Technol.*, 2014, 150527103417002.
- 17 Q. Y. Yue, Q. Li, B. Y. Gao, A. J. Yuan and Y. Wang, *Appl. Clay Sci.*, 2007, **35**, 268.
- 18 J. Febrianto, A. N. Kosasih, J. Sunarso, Y. H. Ju, N. Indraswati and S. Ismadji, *J. Hazard. Mater.*, 2009, **162**, 616.
- 19 R. Song, X. Hu, P. Guan, J. Li, L. Qian, C. Wang and Q. Wang, *Appl. Surf.*, 2015, **332**, 159.
- 20 C. J. Li, S. S. Zhang, J. N. Wang and T. Y. Liu, *Catal. Today*, 2014, **224**, 94.
- 21 H. Quan, H. Li, Z. Huang, T. Zhang and S. Dai, *Int. J. Polym. Sci.*, 2014, **2014**, 1.
- 22 G. Li, L. Zhou, C. Wang and E. Li, *J. Polym. Res.*, 2014, **21**, 523.

